Powder Technology 268 (2014) 139–149

Contents lists available at ScienceDirect

Powder Technology

journal homepage: www.elsevier.com/locate/powtec

The influence of lamellar settler in sedimentation tanks for potable water treatment — A computational fluid dynamic study

Roza Tarpagkou *, Asterios Pantokratoras

Democritus University of Thrace, Department of Civil Engineering, V. Sofias 12, GR-67100 Xanthi, Greece

ARTICLE INFO

Article history:
Received 6 May 2014
Received in revised form 6 August 2014
Accepted 14 August 2014
Available online 23 August 2014

Keywords:
Computational fluid dynamics
Sedimentation
Lamella settling tanks
Multiphase flow
Particle fluid interaction

ABSTRACT

Lamella gravity settlers are often used in water treatment to make sedimentation tanks more cost-effective. Effective surface area for settlement is increased by the inclined plates giving such systems a smaller footprint than the conventional tanks. In this paper a numerical model was used to simulate the dynamics and flow structure of a rectangular sedimentation tank for potable water through a multiphase approach, using computational fluid dynamic (CFD) methods. Two configurations have been examined, one with a system of inclined parallel plates (lamellar settlers) and another with a conventional design, in order to evaluate the influence of lamellar settlers in the process efficiency. Unlike most of the previous numerical investigations which studied the lamellar settlers separately, the present numerical approach studies the whole sedimentation tank with a full scale system of inclined parallel plates. The momentum exchange between the primary and the secondary phase (particles) is taken into account, using a Lagrangian method (discrete phase model) with two-way coupled calculations. Contours of stream function, velocity and concentration are presented, as well as the velocity and concentration profiles for the inclined plates. The results show that the lamellar settlers influence the flow field and increase the sedimentation efficiency by 20% in comparison with the convectional design.

1. Introduction

Sedimentation tanks constitute one of the most common types of water-treatment processing units. They are used in water-treatment facilities in order to remove the majority of the settle-able solids, by the mechanism of gravitational settling. Lamella gravity settlers are often used in water treatment to make rectangular tanks more cost-effective. As in conventional clarifiers, water flows from the bottom of the clarifier and out through the top while particulate settles by gravity to the bottom of the clarifier. The difference between conventional clarifiers and enhanced gravity separators is that the flow in the settling zone is directed through inclined parallel plates or tubes. This virtually eliminates unstable flow patterns and mixing currents, which greatly inhibit the settling of solids. In addition to enhancing laminar flow conditions, the inclined surfaces of the plates reduce the distance that particles need to travel before settling. The particles begin to agglomerate as soon as they hit the surface of the plate, as shown in Fig. 1. The newly created agglomerated particles settle much more rapidly than the fine particles and slide along the settling surface, moving toward the bottom of the clarifier for collection and discharge. Moreover, the efficiency of discrete particle settling in horizontal liquid flow, depends on the area available for settling. The effective surface area for particle settling in enhanced gravity separators is increased by the inclined plates, giving such systems a smaller footprint than the conventional tanks.

Inclined parallel plates are a classical subject with a long history, and Boycott [1] was the first who observed that the settling rate of suspension is better "if the tube is inclined than when it is vertical". This is also known as the Boycott effect. The settling behavior in inclined vessel was modeled firstly by Ponder [2] and latter by Nakamura and Kuroda [3], and for this reason is also known as the PNK theory. According to this theory, the quality of the clarified fluid is a function of the vertical settling velocity of particles and the horizontal projection area of the settler.

In general many researchers have been focused on the study of sedimentation tanks for wastewater treatment. Larsen [4] was probably the first who applied a CFD model to several secondary clarifiers. McCorquodale and Zhou [5] investigated the effect of various solids and hydraulic loads on circular clarifier performance. Patziger et al. [6] investigated the effects of sludge return and the inlet geometry on settling tanks performance.

In a primary sedimentation tank, where the discrete settling prevails, Imam et al. [7] applied a fixed settling velocity and used an averaged particle velocity. Liu et al. [8] conducted measurements and simulations to optimize design of a settling tank.

For potable water treatment Goula et al. [9] modeled a sedimentation tank for potable water and examined the influence of a feed flow control baffle. Tarpagkou and Pantokratoras [10] simulated and examined the effect of particles on fluid phase due to momentum exchange and how this

* Corresponding author. Tel.: +30 25413 00365.
E-mail addresses: rozatarpagou@hotmail.com, rtarpag@civil.duth.gr (R. Tarpagkou).

http://dx.doi.org/10.1016/j.powtec.2014.08.030
0032-5910/

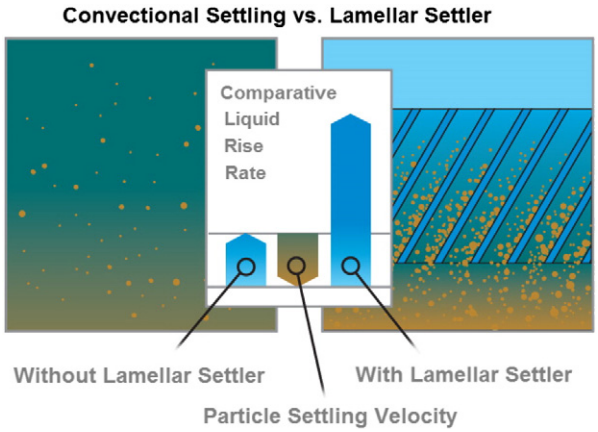

Fig. 1. Particle behavior in conventional settling in comparison with enhanced gravity separators (http://www.brentwoodindustries.com).

affects the fluid velocity. Wang et al. [11] simulated the flow field and SS concentration in a rectangular sedimentation tank.

There are very few theoretical studies about lamellar settlers. Demir [12] used experimental results obtained under different surface loadings and plate angles to evaluate settling tanks. Lekang et al. [13] presented an evaluation of lamellar settling tank using experimental study for measuring inlet and outlet water values of the sedimentation basin. Kowalski and Mięso [14] presented the design of sedimentation tanks and installations utilizing the Boycott's effect. Doroodchi et al. [15] investigated the influence of inclined plates on the expansion behavior of solids suspensions in liquid fluidized beds. Sarkar et al. [16] studied the performance of the inclined plate settlers for aquaculture waste. Rubescu et al. [17] presented a theoretical study concerning the design of lamella secondary settling tank. Galvin et al. [18] examined gravity separation using closely spaced inclined channels. Callen et al. [19] study the particle elutriation from a fluidized bed incorporating parallel inclined plates. Laskovski et al. [20] examine the tendency for particle re-suspension in inclined channels. Lavine [21] examine the mixed convection between inclined parallel plates with a uniform heat flux boundary condition. Okoth et al. [22] summarized the factors which have effect on the separation efficiency of inclined parallel plates, and they modeled the suspension-sediment interaction phenomenologically.

So far, many researchers have used CFD simulations to study water flow and solids removal in settling tanks for sewage water treatment. However, there are not many works in the literature in CFD modeling of sedimentation tanks for potable water treatment. Moreover, according to the authors' best knowledge, the study of the whole sedimentation tank with a full scale system of inclined parallel settlers has never been investigated previously. Unlike most of the previous CFD investigations which studied the lamellar plates separate and alone, the authors believe that this is the first work in the literature which modeled the whole system of sedimentation tank with lamellar settlers for potable water.

The main aim of the present paper is to investigate the 2D hydrodynamics and flow behavior of a rectangular sedimentation tank with two configurations: one with a system of inclined parallel plates (lamellar settlers) and another with a conventional design, in order to evaluate the influence of lamellar settlers in the process efficiency. This was achieved using the computational fluid dynamic (CFD) methods offered by the commercial software ANSYS CFD. The present work fully considers the interaction between the liquid and solid phase (and vice-versa).

The structure of the present paper is the following: in the present section a brief introduction on sedimentation tanks and a brief literature review of previous works have just been conducted. Section 2 presents the mathematical model that is used in the simulations of the present investigation. Section 3 presents the physical problem and the materials and methods that were used in the simulations. It also describes the validation of the proposed numerical model comparing the numerical results with the corresponding experimental data. Section 4 and Section 5 present the results and report the main conclusions drawn from the present study, respectively.

2. Mathematical model

2.1. General information

The hydrodynamic characteristics of a sedimentation tank can be studied as a multiphase flow using either an Euler–Euler or an Euler–Lagrange approach. In the literature, Eulerian applications are used for almost all diffusion dominated problems, but without calculating individually the particle trajectories along the flow field. Due to their versatile capabilities, approaches based on the Lagrangian method have been applied extensively for many two-phase flow problems. The Lagrangian approach provides a more detailed and realistic modeling of particle deposition because the equation that describes the particle motion is solved for each particle moving through the field of random fluid eddies. In such an approach, the fluid is treated as a continuum and the discrete (particle) phase is treated in a natural Lagrangian manner, which may or may not have any coupling effect with the carrying fluid momentum (in the proposed model with coupling effect/two-way coupled calculations). In this paper we used the Euler–Lagrange multiphase approach with two-way coupled calculations which takes into account the interaction between the particles and the fluid (and vice-versa), and calculated the rate of momentum exchanged and transferred from the water to particles (and vice-versa). The main advantage of this approach is that by computing particle trajectories the proposed numerical model can track the momentum gained or lost by the particle stream that follows that trajectory and these quantities can be incorporated in the subsequent continuous phase calculations. Thus, while the continuous phase always impacts with the discrete phase, in this model we incorporated the effect of the discrete phase trajectories on the continuum. This interchange affects fluid velocity, especially in the case of large particle sizes, which have a greater relaxation time in relation to the characteristic time of the tank [10].

In the case of turbulent flows, the conservation equations are solved to obtain time-averaged information. Since the time-averaged equations contain additional terms, which represent the transport of mass and momentum by turbulence, turbulence models that are based on a combination of empiricism and theoretical considerations are introduced to calculate these quantities from details of the mean flow.

In the simulations of the current work the RNG k–ε model is applied for turbulence closure. This model was derived using a rigorous statistical technique, the renormalization group theory. The basic form of the RNG k–ε model is similar to the standard k–ε model, but it includes a number of refinements, rendering it more appropriate for the numerical simulations of the present investigation, as it is more accurate for swirling flows and rapidly strained flows and also accounts for low Reynolds number effects. Moreover, it provides an analytical formula for the calculation of the turbulent Prandtl numbers. At this point it should be mentioned that the RNG k–ε model is also modified accordingly in order to simultaneously account for the primary (continuous) phase and the secondary (dispersed) phase of the simulated flows.

2.2. Governing equations

2.2.1. Fluid phase

Fluid phase is treated as a continuum by solving the Navier–Stokes equations so the equations of conservation of mass (Eq. (1)) and

momentum (Eq. (2)) in the case of incompressible, stationary turbulence can be written in Cartesian-tensor notation as:

$$\frac{\partial u_i}{\partial x_i} = 0 \tag{1}$$

$$U_j \frac{\partial U_i}{\partial x_j} = -\frac{1}{\rho}\frac{\partial p}{\partial x_i} + \frac{\partial}{\partial x_j}\left(\nu\left(\frac{\partial U_i}{\partial x_j} + \frac{\partial U_j}{\partial x_i}\right) - \overline{u_i'}\overline{u_j'}\right) \tag{2}$$

where p is the static pressure, ν is the kinematic viscosity, u_i denotes the instantaneous velocity associated with the x_i coordinate direction, while U_i is the average, mean flow velocity and u_i' is the turbulent velocity fluctuation such that $u_i = U_i + u_i'$. The term $\overline{u_i'}\overline{u_j'}$, which is known as Reynolds-stress tensor, has to be determined with a turbulence closure model.

2.2.2. Turbulence

The general transport equations for the turbulence kinetic energy k and the turbulence dissipation rate ε, of the RNG k–ε turbulence model, can be described by Eq. (3) and Eq. (4) respectively:

$$\frac{\partial}{\partial x_i}(\rho k u_i) = \frac{\partial}{\partial x_j}\left(a_k \mu_{eff}\frac{\partial k}{\partial x_j}\right) + G_k + G_b - \rho\varepsilon \tag{3}$$

$$\frac{\partial}{\partial x_i}(\rho \varepsilon u_i) = \frac{\partial}{\partial x_j}\left(a_\varepsilon \mu_{eff}\frac{\partial \varepsilon}{\partial x_j}\right) + C_{1\varepsilon}\frac{\varepsilon}{k}(G_k + C_{3\varepsilon}G_b) - C_{2\varepsilon}\rho\frac{\varepsilon^2}{k} - R_\varepsilon \tag{4}$$

where G_k is the generation of turbulence kinetic energy due to mean velocity gradients, G_b is the generation of turbulence kinetic energy due to buoyancy, a_k and a_ε are the inverse effective Prandtl numbers for k and ε respectively, μ_{eff} is the effective viscosity and $C_{1\varepsilon}$, $C_{2\varepsilon}$ and $C_{3\varepsilon}$ are turbulence model constants. The term R_ε in the ε equation accounts for the effects of rapid strain and streamline curvature which plays an important role in the anisotropy of the large-scale eddies.

2.2.3. Equation of particle motion

The proposed model predicts the trajectory of a discrete phase particle by integrating the force balance on the particle, which is written in a Lagrangian reference frame. This force balance equates the particle inertia with the forces acting on the particle, and can be written as:

$$m_p\left(\frac{du_p}{dt}\right) = m_p F_D\left(u - u_p\right) + m_f\left(\frac{Du}{Dt}\right) + \frac{1}{2}m_f\left(\frac{Du}{Dt} - \frac{du_p}{dt}\right) + \left(m_p - m_f\right)g + \frac{1}{2}\left(\pi\rho_p r^2\right)C_L L V^2 \tag{5}$$

where d/d t is the derivative with respect to time following the moving particle, D/Dt is the total acceleration of the continuous phase as seen by the particle, u_p is the velocity of the particle and u is the velocity of the continuous phase, u_p is the mass of the particle, m_f is the mass of the fluid displaced by the particle, g is gravity acceleration, r is the radius of the particle, ρ_p is the density of the dispersed phase, C_L is the lift coefficient evaluated by Saffman, L is the directional cosine, V represents the magnitude of the relative velocity vector, $F_D(u - u_p)$ is the drag force per unit particle mass, where:

$$F_D = \frac{18\mu}{\rho_p d_p^2}\frac{C_D \mathrm{Re}}{24}. \tag{6}$$

Here d_p is the particle diameter, μ is the dynamic viscosity of the continuous phase, C_D is the drag coefficient as a function of Reynolds number $\{C_D = f(\mathrm{Re})\}$ according to the known relation for spherical particles. The relative Reynolds number is defined as:

$$\mathrm{Re} = \frac{\rho d_p \left|u_p - u\right|}{\mu} \tag{7}$$

where ρ is the density of the fluid. The term on the left hand side of Eq. (5) is the inertia force acting on the particle due to its acceleration. The terms on the right hand side are respectively, forces due to viscous and pressure drag, the force due to the fluid pressure gradient and viscous stresses, the inertia force of the added or virtual mass, the buoyancy force, and the Saffman lift force due to shear in the carrier flow.

2.2.4. Momentum exchange

As mentioned previously, in the present investigation the discrete phase model (Lagrangian approach) with coupled momentum calculations is used. In other words a momentum exchange between the primary and the secondary phase and vice-versa, takes place during the calculations. As the trajectory of a particle is computed, the model keeps track of the momentum gained or lost by the particle stream that follows that trajectory and these quantities can be incorporated in the subsequent continuous phase calculations.

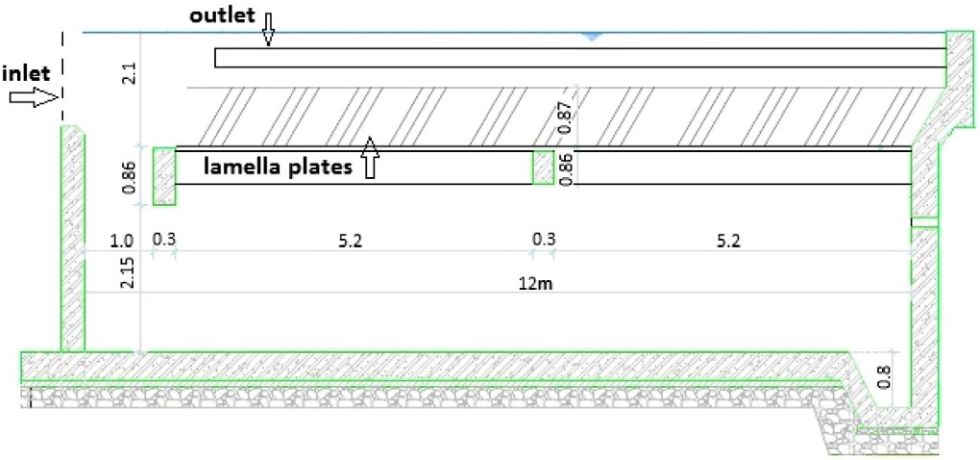

Fig. 2. Geometry of the physical problem.

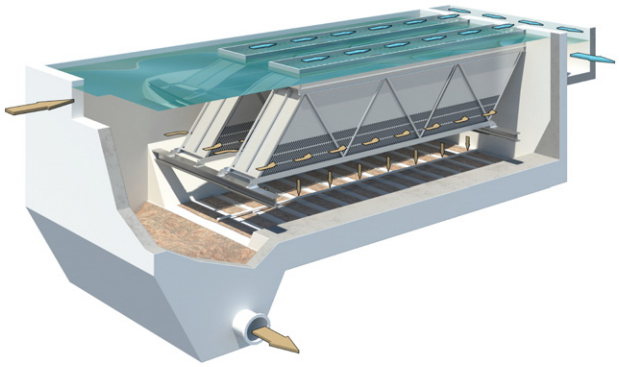

Fig. 3. Inclined plate installation.
Reprinted from Nordic Water, Lamella Settlers brochure, with permission from Nordic Water.

The momentum transfer from the continuous phase to the discrete phase is computed by examining the change in momentum of a particle as it passes through each control volume in the CFD model.

This momentum change is computed as:

$$F = \sum\left(\frac{18\mu C_D \mathrm{Re}}{\rho_p d_p^2 24}\left(u_p - u\right) + F_{other}\right)m_p \Delta t \tag{8}$$

where Δt is the time step and F_{other} represents the other interaction forces.

2.3. Computational fluid dynamic boundary conditions

At inlets, a velocity-inlet boundary condition is used. With this type of boundary condition, a uniform distribution of all the dependent variables is prescribed at the face representing the sediment laden water inflow. In more detail, the velocity magnitudes of the primary and secondary phases with directions normal to the inlet face are specified, assuming constant, uniform values. For the outlets, a pressure-outlet boundary condition is applied. Using this type of boundary condition, all flow quantities at the outlets are extrapolated from the flow in the interior domain. A set of "backflow" conditions can be also specified, allowing reverse direction flow at the pressure outlet boundary during the solution process. At the free ambient water surface, a symmetry boundary condition is used. The solid boundaries are specified as stationary walls with a no-slip shear condition.

For the discrete phase model the additional boundary conditions are: for the velocity inlet and pressure outlet an "escape" condition is prescribed. This means that the particle is reported as having escaped when it encounters the boundary in question and this is assumed in all flow boundaries. Near the solid boundaries a "reflect" condition is prescribed. This means that the particle rebounds off the boundary in question with a change in its momentum as defined by the coefficient of restitution. Finally, at the bottom of the tank a "trapped" condition is used. This means that the trajectory calculations are terminated and the state of the particle is recorded as trapped when it encounters the proposed boundary.

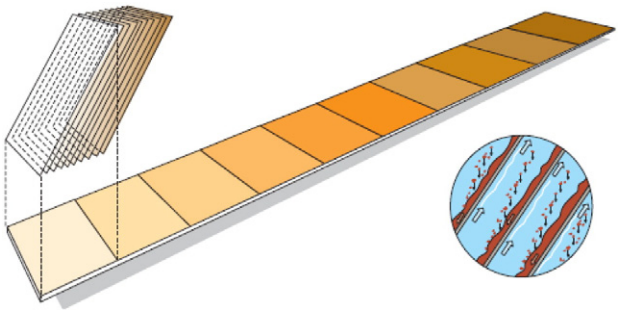

Fig. 4. Lamella settlers reduce the footprint of the tank.
Reprinted from Nordic Water, Lamella Settlers brochure, with permission from Nordic Water.

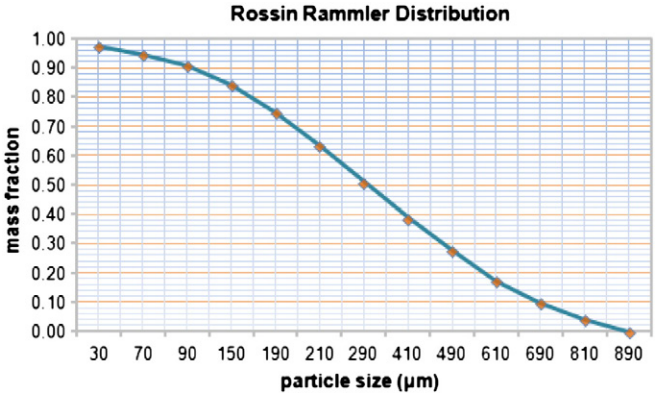

Fig. 5. Range of particle diameters for the Rosin–Rammler distribution.

2.4. Solution procedure

The Euler–Lagrange multiphase approach predicts the trajectory of a discrete phase particle by integrating the force balance on the particle, which is written in a Lagrangian reference frame. This force balance equates the particle inertia with the forces acting on the particle, and can be written (for the x direction in Cartesian coordinates) as

$$\frac{du_p}{dt} = F\left(u - u_p\right) + \frac{g_x\left(\rho_p - \rho\right)}{\rho_p} + F_x \tag{9}$$

where F_x is an additional acceleration (force/unit particle mass) term. The trajectory equations are solved by stepwise integration over discrete time steps. The velocity of the particle at each point along the trajectory, with the trajectory itself predicted by

$$\frac{dx}{dt} = u_P. \tag{10}$$

As mentioned previously, we incorporated the effect of the discrete phase trajectories on the continuum. This two-way coupling is accomplished by alternately solving the discrete and continuous phase equations until the solutions in both phases have stopped changing. The strategy that is followed during the solution procedure can be summarized in the following steps:

Table 1
Sample characteristics for the Rosin–Rammler distribution.

Class	Range of particle size (μm)	Mean particle size (μm)	Mass fraction	d	Υ_d	n
1	10–30	20	0.025	30	0.975	1.504524
2	30–70	50	0.027	70	0.948	1.835608
3	70–90	80	0.038	90	0.91	1.755707
4	90–150	120	0.067	150	0.843	2.119042
5	150–190	170	0.094	190	0.749	2.076975
6	190–210	200	0.114	210	0.635	1.586513
7	210–290	250	0.125	290	0.51	2.262864
8	290–410	350	0.123	410	0.387	−0.3032
9	410–490	450	0.112	490	0.275	0.730257
10	490–610	550	0.101	610	0.174	0.982546
11	610–690	650	0.077	690	0.097	1.224182
12	690–810	750	0.057	810	0.04	1.371499
13	810–890	850	0.04	890	0	0
		345.3846154	1			1.428876

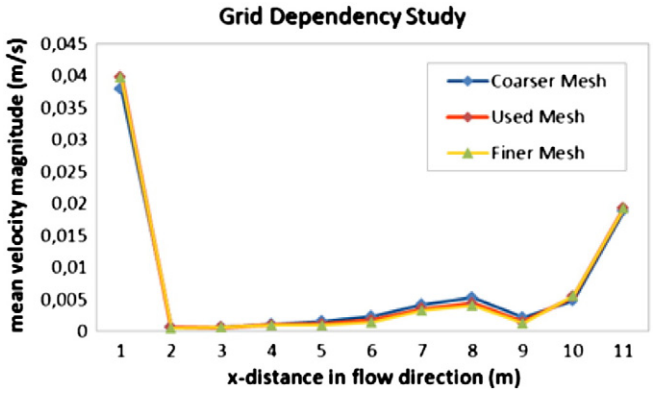

Fig. 6. Grid dependency study.

1. The continuous phase flow field is solved prior to the introduction of the discrete phase.
2. The discrete phase is introduced by calculating the particle trajectories for each discrete phase injection.
3. The continuous phase flow is recalculated, taking into consideration the momentum interphase exchange, the heat and the mass that was determined during the previous step.
4. The discrete phase trajectories are then recalculated in the modified continuous phase flow field.
5. Steps 3 and 4 are repeated until a converged solution is achieved, where both the continuous phase flow field and the discrete phase particle trajectories do not change with any additional calculation. The coupled procedure must be followed in order to include the important impact of the discrete phase on the continuous phase flow field.

3. Description of numerical application

3.1. Physical problem

In the present paper the rectangular sedimentation tank for potable water treatment plant which is to be constructed in the city of Thessaloniki was investigated. The plant receives raw water from Aliakmon River and its capacity is 150,000 m^3/day. The employed processes include pre-ozonation, coagulation–flocculation, sedimentation, sludge thickening, filtration through sand and active carbon, ozonation and chlorination. The sedimentation tank is being supplied through a rectangular channel 1.1 m wide. The outlet of water from the sedimentation is via 7 perforated pipes (PVC DN 10 atm), as can be seen in Fig. 2.

Within the settling chamber inclined parallel plates with an inclination angle of 60° are contained to enable a larger settling area for the decantation of suspended solids (lamellar settlers). The inclined plates have a thickness of 1.2 mm, a height of 1 m and are spaced 50 mm apart. The inclined plates rely on concrete beams as shown in Fig. 3.

This design allows particles to settle more rapidly by achieving laminar flow and also by decreasing the distance a particle needs to travel before it is considered a settled particle. Instead of traveling several feet to the bottom of the tank, it now must only travel a few inches or less. This rapid settling effect maximizes the effective surface area for settling and therefore it minimizes the clarifier footprint, as can be seen in Fig. 4.

In addition, the hydraulic design ensures equal flow distribution over the lamella plates to enhance separation. Flow passes through the inlet channel to the settling zone and proceeds upward through the plates. As the liquid flows upward, the solids settle on the inclined parallel plates (shown in Fig. 4) and slide into the sludge hopper at the bottom.

Two cases have been examined: one with a system of inclined parallel plates (lamellar settlers, shown in Fig. 2) and another with a conventional design, in order to evaluate the influence of lamellar settlers in the process efficiency.

3.2. Simulation-computational procedure

The continuous phase flow field is firstly solved in the absence of particles. The converged solution was defined as the solution for which the normalized residuals for all variables were less than 10^{-4}. Then the particles are released from the inlet and are tracked along their trajectories. Finally recalculation of the continuous flow field, using the interphase exchange of momentum (two-way coupled calculation) until a converged solution is achieved in both the continuous and discrete particle phase, takes place.

In order to account for turbulent dispersion, the stochastic tracking of particles due to turbulence eddies was determined using the discrete "random walk model" (this turbulence model uses a Gaussian probability distribution and a turbulence viscosity from CFD results to simulate the impact of velocity fluctuations on the particle trajectories), in conjunction with RNG k–ε model. The effect of lift forces in the secondary phase solid particles is also taken into account, in the calculations of the present investigation.

The inlet flow velocity used was 0.023 m/s. The particle density used was 1066 kg/m^3 and the range of particle size was 30–890 μm and followed the Rosin–Rammler distribution. Rosin–Rammler distribution is a convenient representation of the particle size distribution. The complete range of sizes is divided into an adequate number of discrete

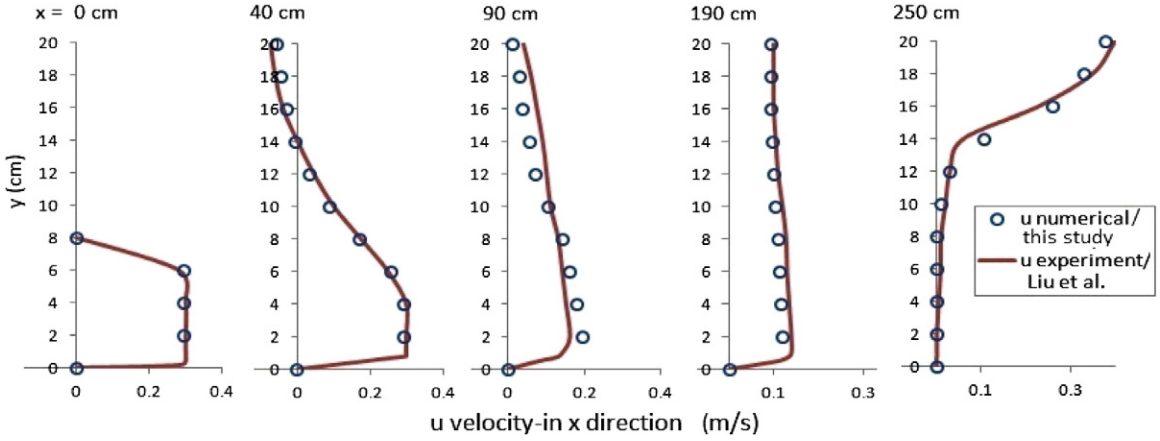

Fig. 7. Comparisons of the experimental data [8] with the numerical results of ANSYS code.

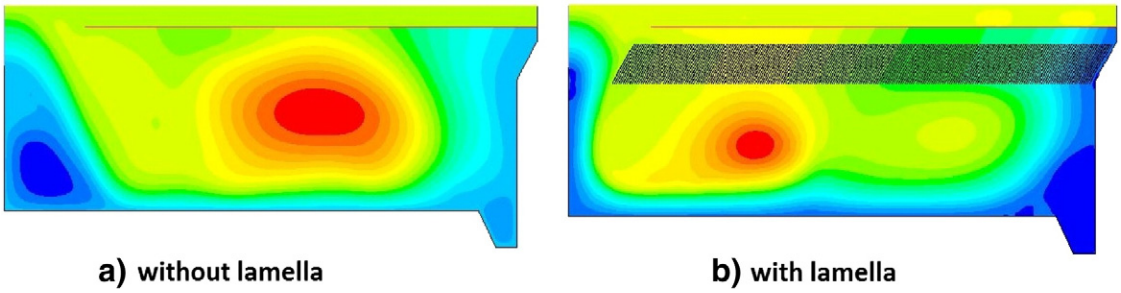

Fig. 8. Streamline contours for a) conventional design and b) design with lamellar settlers.

intervals; each represented by a mean diameter for which trajectory calculations are performed. Fig. 5 and Table 1 show the characteristics of the sample for this distribution, where Y_d is the mass fraction of particles of diameter greater than d:

$$Y_d = e^{-(d/\bar{d})^n} \tag{11}$$

where n is the size distribution parameter.

The computational mesh used in the simulations for all of the above cases consists of a total number of 218,821 cells. In order to ensure that the solution is mesh-independent, two additional meshes were used, one coarser consisting of 135,710 cells and a finer one consisting of 581,933 cells. In Fig. 6 the mean velocity magnitude versus distance in the flow direction is depicted indicatively for those three meshes. As it can be seen the resulting graphs compare very well and the maximum difference between the predictions made by the selected, coarser and finer grids was 3.2%. Therefore, the solution with the grid of 218,821 elements is considered to be mesh-independent.

3.3. Model validation

Specific experimental quantitative results of velocity measurements are compared with the corresponding numerical results, in order to validate the reliability of the ANSYS Fluent code. This was achieved by simulating the velocity measurements of Liu et al. [8]. The velocity measurements of Liu et al. [8] have been taken in a rectangular sedimentation tank for several inlet and flow rate configurations. The comparison of the numerical model (Fluent) concerns the velocity measurements of the case 3 in the work of Liu et al. [8], which corresponds to a flow with Re = 22,239 (transitional flow). The RNG k–ε model is applied for turbulence closure in the numerical simulations. The numerical velocity profiles and the corresponding experimental data are illustrated in Fig. 7 and the comparison is very good.

4. Results and discussions

4.1. Macroscopic observations

The most important macroscopic observation drawn from this study is the influence of lamellar settlers on the flow field. In Fig. 8 streamlines for a) conventional design and b) design with lamellar settlers are depicted. In the case of the convectional design a large recirculation eddy has been produced at the center of the tank, and two small vortices have been created, one below the inlet and another near the hopper. In the case with the inclined parallel plate system the central vortex has been divided into two smaller vortices. The vortex below the inlet is now smaller and placed exactly below the inlet channel in contrast to the vortex near the hopper which is now bigger than in the case of the conventional design. From all of the above it is clear that the existence of lamellar settlers has a significant influence on the vortex formation.

Fig. 9 shows the contours of velocity for the convectional design and for the design with lamellar settlers. In general, fluid velocity is higher in the case of the convectional tank. The reason for this phenomenon is that in the tank with the lamellar settlers more particles are trapped in the bottom or in the inclined plates (as can be seen in Fig. 10 where concentration contours are depicted) and the remaining concentration is lower within the tank. On the contrary, in the conventional tank, more particles are levitated, and thus the concentration is higher. This influences the path of the fluid, and as a consequence, the fluid velocity increases. The phenomenon of velocity increase in regions with high particle concentrations has been also observed by Kulick et al. [23].

In Fig. 10 concentrations (kg/m^3) for a) conventional design and b) design with lamellar settlers are depicted. In the case of the conventional design the particles are diffused into the tank and a large amount of particles are directed in the perforated pipe. The tank efficiency is in

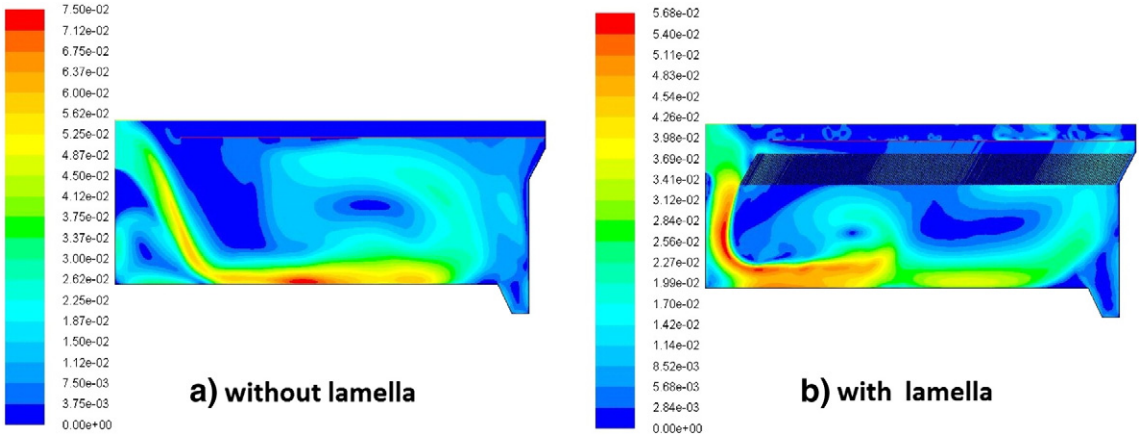

Fig. 9. Velocity contours (m/s) for a) conventional design and b) design with lamellar settlers.

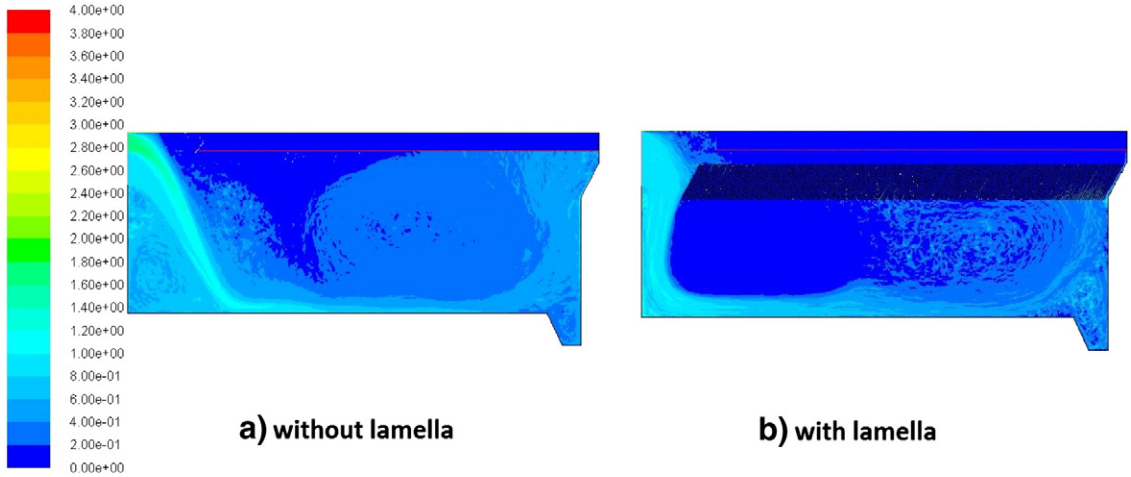

Fig. 10. Concentration contours (kg/m^3) for a) conventional design and b) design with lamellar settlers.

this case 75% (The effectiveness of particle settling is estimated as the percentage of solids settled over the rate of solids introduced from the feed.). In the case of the design with the lamellar settlers the amount of particles which haven't settled into the bottom goes up to the inclined parallel plates with the majority of particles being trapped in the lamellar settlers. As a consequence, the percentage of particles which escape from the perforated pipe is significantly lower with the tank efficiency to reach in this case up to 93%.

4.2. Quantitative results

The flow between the parallel inclined plates in the case of the design with lamellar settlers was studied thoroughly. Concentration profiles were extracted for three inclined plates: the first, the middle and the last lamella are depicted in Fig. 11. In each of these inclined plates three concentration profiles were extracted: one at the inlet, one at the middle and one at the outlet position of each lamella.

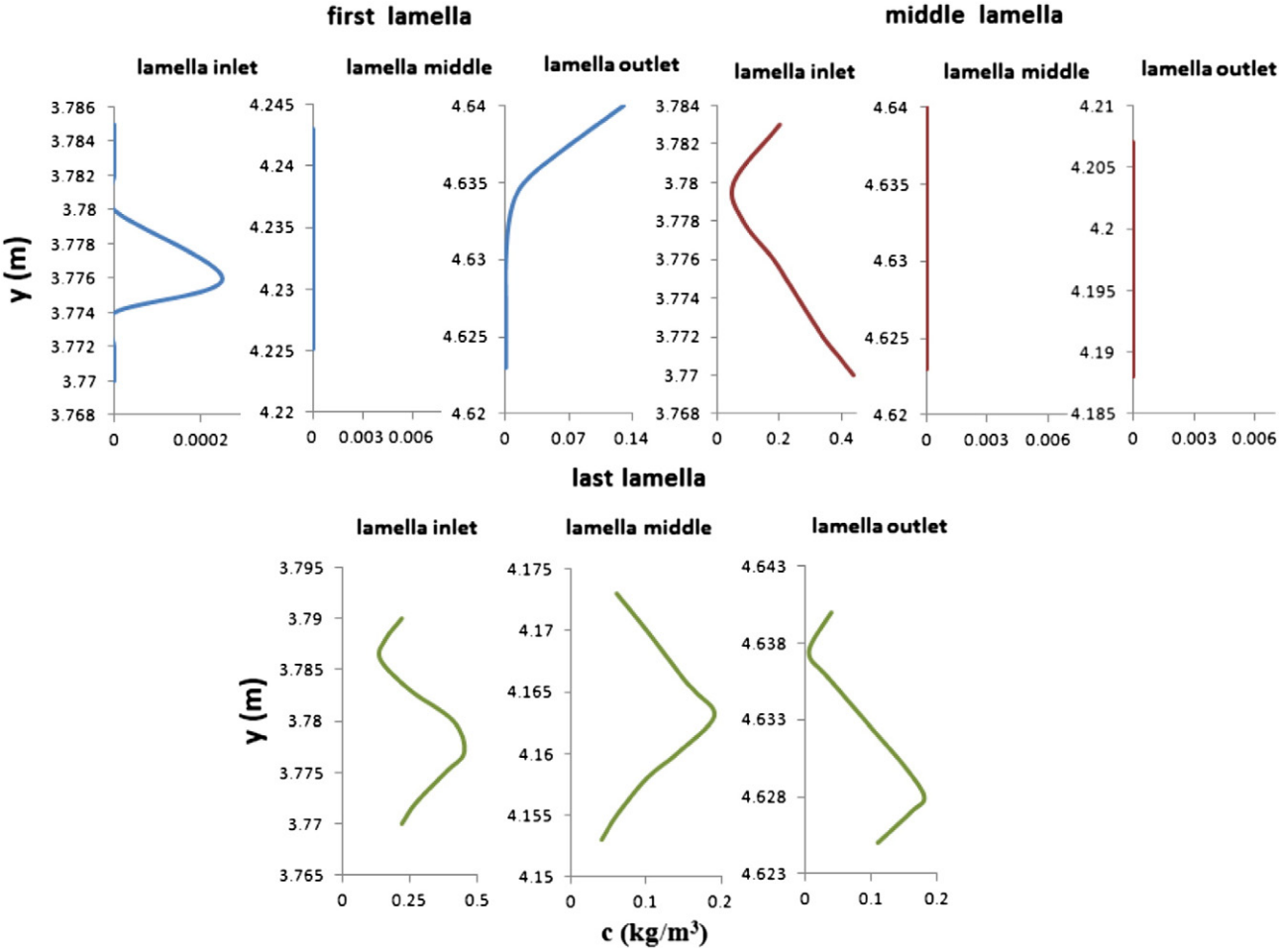

Fig. 11. Concentration profiles (kg/m^3) in the inclined parallel plates.

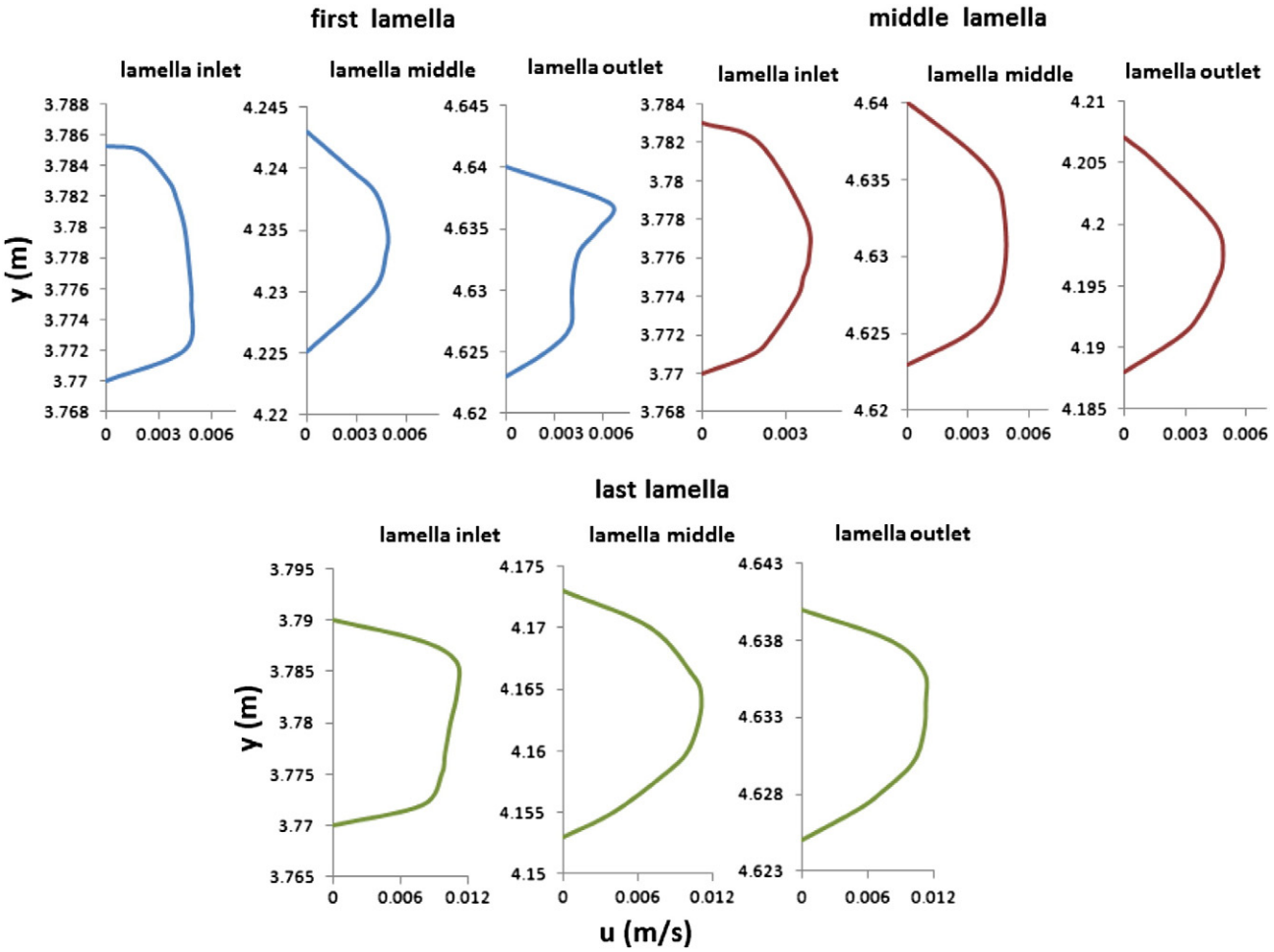

Fig. 12. Velocity profiles (u, m/s) in the inclined parallel plates.

4.2.1. First lamella

In the position of the first lamella a backflow has been generated. The particles are not able to descent before the inclined plate and as a consequence descend through the lamella. In this first lamella there appears the phenomenon that the flow enters from the lamella end (lamella outlet) and exits from lamella inlet. For that reason the concentration at the end of the first lamella is higher and smaller at the inlet and as the flow descends through the inclined plate, a high percentage of particles is trapped on the plates.

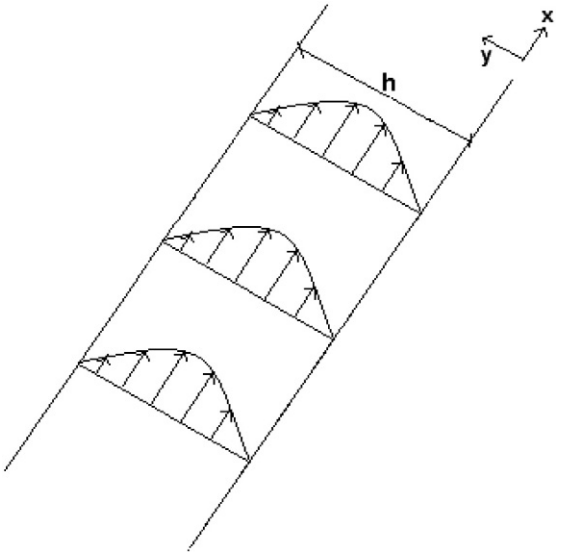

Fig. 13. Classical problem of the fluid flow through parallel inclined plates.

4.2.2. Middle lamella

In the position of the middle lamella the flow is now directed upward to the inclined parallel plates normally, and through them directed to the perforated pipe. The remaining particles which have not settled to the bottom enter into the lamella inlet, and in this position the concentration is high. As the liquid flows upward, the majority of the particles settle on the inclined parallel plates and for that reason the concentration decreases and becomes zero at the lamella outlet. This indicates that the water exiting from the lamellar settler is in this position actually is clear from particles, and the central inclined parallel plates withhold the 100% of the particles which enters in them.

4.2.3. Last lamella

In the position of the last lamella the flow is again directed upward to the inclined parallel plates normally, and through them directed to the perforated pipe. The remaining particles which have not settled to the bottom enter into the lamella inlet, and in this position the concentration is high. A large amount of particles settle in the plates and the concentration decreases in the direction of the lamella outlet. In this position the lamellar settler withholds 65% of the particles which enters in them.

In Fig. 12 velocity profiles are depicted for the same three inclined plates: the first, the middle and the last lamella. In each of these

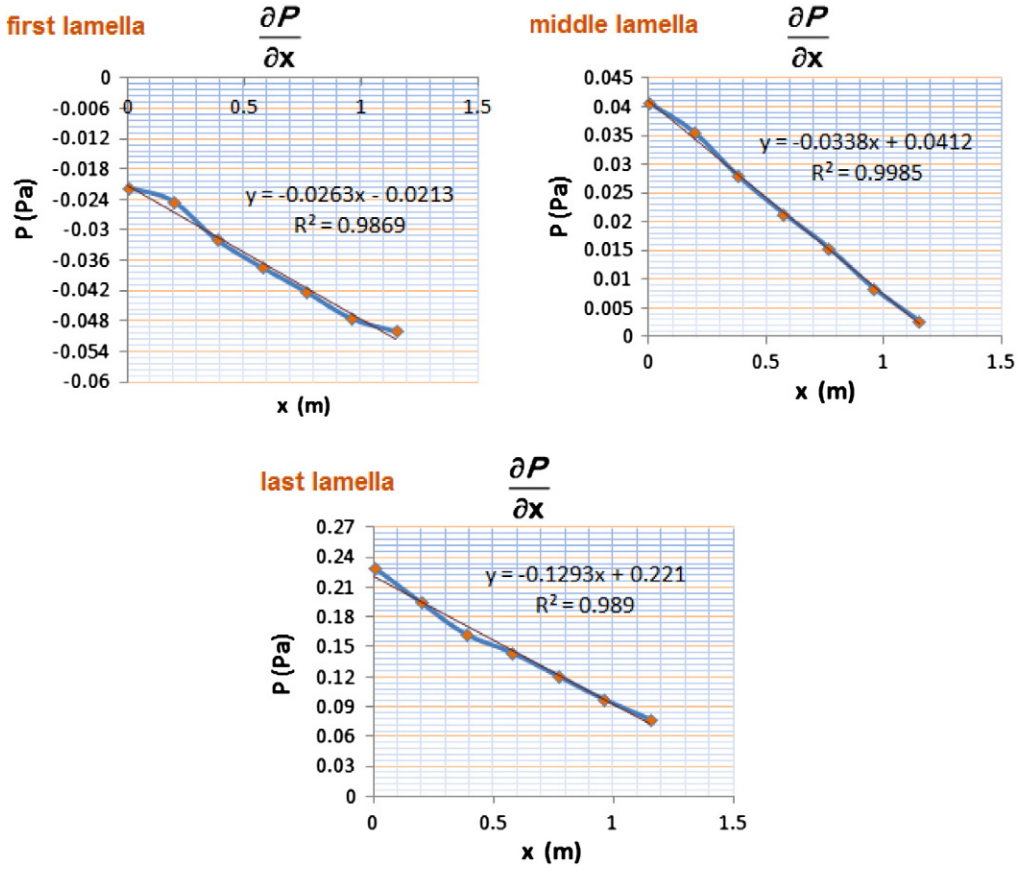

Fig. 14. Variations of pressure with respect to x axis (on the inclined parallel plate coordinate system), as they result from the simulations.

inclined plates three velocity profiles were extracted: one at the inlet, one at the middle and one at the outlet position of each lamella. As mentioned above, the middle inclined plates withhold 100% and the latter withhold 65% of the particles which enters in them. This can be explained by studying Fig. 9b, where fluid velocity increases at the position of the latter plates. This velocity increase is even more evident by observing Fig. 12, where fluid velocity at the inlet position of the last lamella is four times higher than fluid velocity at the inlet position of the middle lamella. For that reason the particle sedimentation is higher at the middle lamella in contrast to the last lamella, where water moves faster, drags particles along and a percentage of the particles was unable to settle.

The flow between the lamellar settlers (parallel inclined plates) is actually like the Poiseuille flow between parallel plates and was studied thoroughly. In Fig. 13 the classical problem of the fluid flow through parallel inclined plates, is depicted. The velocity profiles from lamella settlers (Fig. 12) are similar to those on Poiseuille flow, but lamellar settlers are not long enough to get the perfect parabolic profile. From Navier–Stokes equations the general-state solution for fully developed Poiseuille flow is:

$$u_x(y) = \frac{y(y-h)}{2\mu}\frac{\partial P}{\partial x}. \tag{12}$$

Fig. 14 shows the variations of pressure with respect to x axis (on the inclined parallel plate coordinate system), and as a consequence the partial derivative of pressure with respect to x axis, for the first, the middle and the last lamella, as they result from the simulations of the numerical model. The component of gravity on x axis has already been incorporated from the computational model in the pressure term.

Specific quantitative results from the numerical model (Fluent) and from analytical solution for Poiseuille flow (Eq. (12)) are compared in Table 2; for the first, middle and last lamella, for the middle y position (u_{max}). The partial derivative of pressure with respect to x axis, for Eq. (12), resulting from Fig. 14. The fluid flow profiles of the lamellar settles matching very well with Poiseuille flow, since the maximum difference does not exceed 5%. In addition, this good convergence between the analytical solution and the numerical code is a further proof that the numerical model (Fluent) gives accurate results and captures the flow field inside the parallel plates.

Fig. 15 depicts particle concentration (kg/m^3) at the bottom of the tank and at the perforated outlet pipe, for the two simulated configurations: the conventional design and the design with lamellar settlers. In the design with the lamellar settlers the particle concentration is higher at the bottom in contrast to the convectional design. This indicates that less suspended solids directed to the outlet pipe. In this design the remaining particles which were not able to settle at the bottom are directed toward to the inclined parallel plates and slide into the sludge hopper at the bottom again. The most important observation though, is that at the perforated outlet pipe the particle concentration is lower for the design with lamellar settlers compared to the conventional design. This suggests that less suspended solids are directed to the outlet

Table 2
Quantitative velocity comparisons between the numerical model (Fluent) and the analytical solution for Poiseuille flow for the middle y position (u_{max}).

u (m/s)	First lamella	Middle lamella	Last lamella
Numerical model (Fluent)	0.00478	0.0049	0.0115
$\frac{\partial P}{\partial x}$	−0.0263	−0.0338	−0.1993
Analytical solution for Poiseuille flow	0.00454	0.0051	0.012
Δu%	5%	4%	4.16%

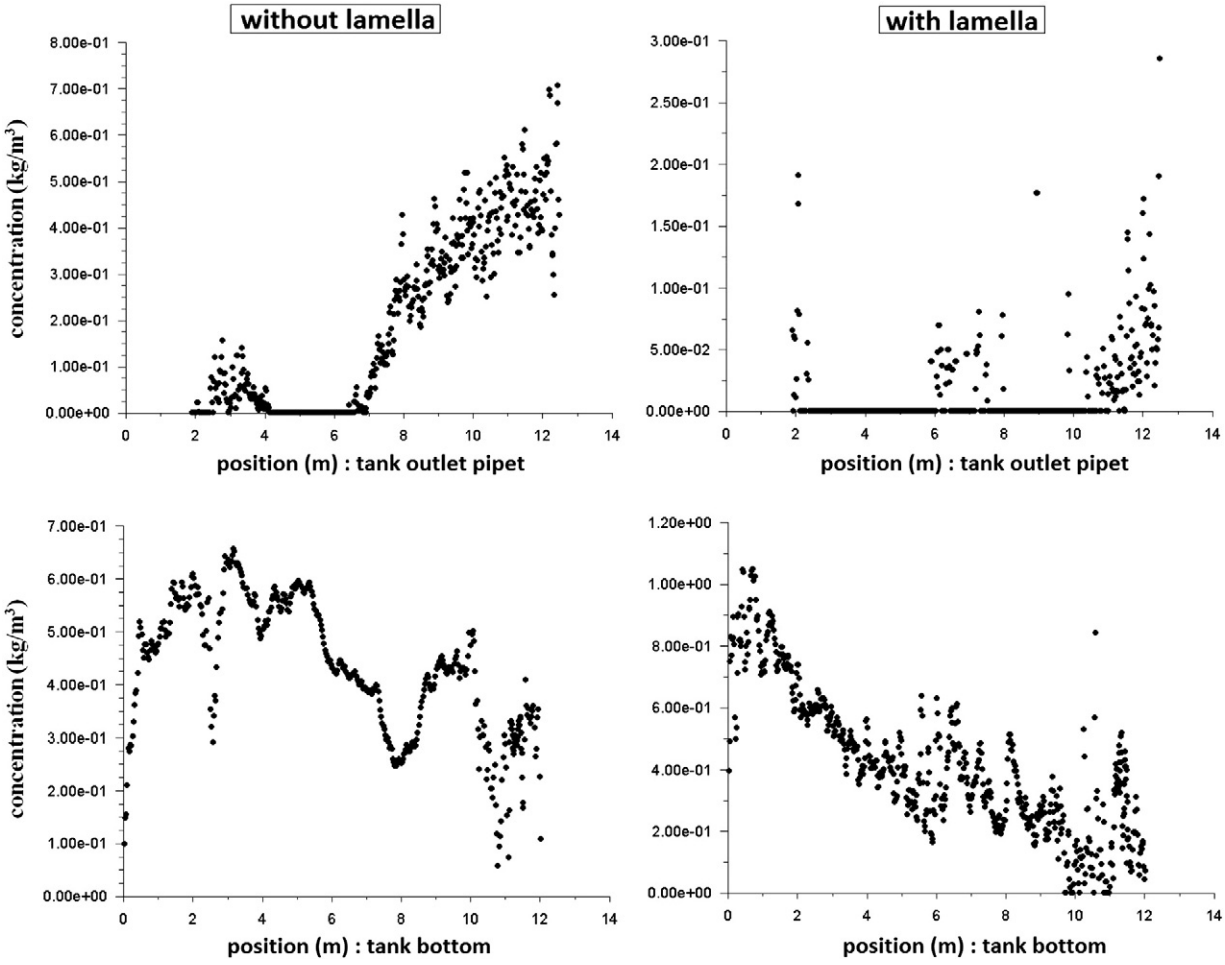

Fig. 15. Particle concentration (kg/m^3) for a) conventional design and b) design with lamellar settlers, at the bottom of the tank and at the perforated outlet pipe.

pipe, since the lamellar settler withhold an substantial amount of them and the rest slide into the sludge hopper at the bottom again, and the overall sedimentation efficiency is of the order of 93%. At the conventional design the suspended solids directed toward to the outlet pipe and the overall sedimentation efficiency is of the order of 75%. Moreover, the particle concentration has decreased along the *y* axis (from the bottom to the outlet pipe) in the case of the conventional design only by 14%. In the case of the design with the parallel inclined plates the particle concentration has decreased along the *y* axis by 75% due to lamellar settlers.

Considering all of the above it is clear that the installation of the lamellar settlers increases the settling, making the rectangular tank more efficient and more cost-effective.

5. Conclusions

In this paper a numerical model was used to simulate the dynamics and flow structure of a rectangular sedimentation tank with lamellar settlers for potable water through a multiphase approach. The flow of the tank has been simulated with the ANSYS Fluent CFD code. Unlike most of the previous numerical investigations which studied the lamellar settlers separate and alone, the present numerical approach studies the whole sedimentation tank with a full scale system of inclined parallel plates. Two configurations have been examined, one with a system of inclined parallel plates (lamellar settlers) and another with a conventional design, in order to evaluate the influence of lamellar settlers in the process efficiency. The interaction between the liquid and solid phase (and vice-versa) was implemented within the model. The proposed numerical approach is tested and verified through detailed qualitative and quantitative comparisons with experimental data.

The following conclusions have been derived:

1. In the design with the lamellar settlers the particle concentration is higher at the bottom. In this design the remaining particles which were not able to settle at the bottom directed toward to the inclined parallel plates and slide into the sludge hopper at the bottom again. For that reason the particle concentration is lower at the perforated outlet pipe and has decreased along the *y* axis (from the bottom to the outlet pipe) by 75%. In this case the overall sedimentation efficiency of the tank is of the order of 93%.
2. In the conventional design the particle concentration is lower at the bottom, in contrast to the lamellar settlers design. The suspended solids directed toward the outlet pipe and the particle concentration has decreased along the *y* axis (from the bottom to the outlet pipe) in the case of the convectional design only by 14%. In this case the overall sedimentation efficiency of the tank is in the order of 75%.
3. The effective surface area for settlement is increased by the inclined plates giving a smaller footprint than in the conventional tank, and the installation of the lamellar settlers make the rectangular tank more efficient and more cost-effective.

Acknowledgments

The financial support provided by the Thessaloniki Water Supply and Sewerage Co. (EYATH) SA (KE 2133/80837) is gratefully acknowledged.

The authors would like to thank K. Zampetoglou, G. Seretoudi, A. Soupila, A. Papaionannou and E. Samara for their contribution.

References

[1] A.E. Boycott, Sedimentation of blood corpuscles, Nature (1920) 104–532.
[2] E. Ponder, On sedimentation and rouleaux formation, Q. J. Exp. Physiol. 15 (1925) 235–252.
[3] N. Nakamura, K. Kuroda, La cause de l'acceleration de la vitesse de sedimentation de suspensions dans les recipients inclines, Keijo J. Med. 8 (1937) 256–296.
[4] P. Larsen, On the hydraulics of rectangular settling basins, Rep. No. 1001, Dept. of Water Research Engineering, Lund Institute of Technology, Lund, Sweden, 1977.
[5] J.A. McCorquodale, S. Zhou, Effects of hydraulic and solids loading on clarifier performance, J. Hydraul. Res. 31 (1993) 461–477.
[6] M. Patziger, H. Kainz, M. Hunze, J. Jozsa, Influence of secondary settling tank performance on suspended solids mass balance in activated sludge systems, Water Res. 46 (2012) 2415–2424.
[7] E. Imam, J.A. McCorquodale, J.K. Bewtra, Numerical modeling of sedimentation tanks, J. Hydraul. Eng. ASCE 109 (1983) 1740–1754.
[8] B. Liu, J. Ma, L. Luo, Y. Bai, S. Wang, J. Zhang, Two-dimensional LDV measurement, modeling, and optimal design of rectangular primary settling tanks, J. Environ. Eng. ASCE 136 (2010) 501–507.
[9] A.M. Goula, M. Kostoglou, T.D. Karapantsios, A.I. Zouboulis, A CFD methodology for the design of sedimentation tanks in potable water treatment case study: the influence of a feed flow control baffle, Chem. Eng. J. 140 (2008) 110–121.
[10] R. Tarpagkou, A. Pantokratoras, CFD methodology for sedimentation tanks: the effect of secondary phase on fluid phase using DPM coupled calculations, Appl. Math. Model. 37 (2013) 3478–3494.
[11] X. Wang, L. Yang, Y. Sun, L. Song, M. Zhang, Y. Cao, Three-dimensional simulation on the water flow field and suspended solids concentration in the rectangular sedimentation tank, J. Environ. Eng. ASCE 134 (2008) 902–911.
[12] A. Demir, Determination of settling efficiency and optimum plate angle for plated settling tanks, Water Res. 29 (1995) 611–616.
[13] O.I. Lekang, A.M. Bomo, I. Svendsen, Biological lamella sedimentation used for wastewater treatment, Aquac. Eng. 24 (2001) 115–127.
[14] W.P. Kowalski, R. Mięso, Cross-current lamella sedimentation tanks, Archives of civil and mechanical engineering IV (2004) 5–26.
[15] E. Doroodchi, K.P. Galvin, D.F. Fletcher, The influence of inclined plates on expansion behaviour of solid suspensions in a liquid fluidised bed—a computational fluid dynamics study, Powder Technol. 156 (2005) 1–7.
[16] S. Sarkar, D. Kamilya, B.C. Mal, Effect of geometric and process variables on the performance of inclined plate settlers in treating aquacultural waste, Water Res. 41 (2007) 993–1000.
[17] D. Rubescu, C. Mandis, D. Rubescu, Design lamellar secondary settling tank using numerical modeling, U.P.B. Sci. Bull. 74 (2010) 211–216.
[18] K.P. Galvin, J. Zhou, K. Walton, Application of closely spaced inclined channels in gravity separation of fine particles, Miner. Eng. 23 (2010) 326–338.
[19] A. Callen, B. Moghtaderi, K.P. Galvin, Use of parallel inclined plates to control elutriation from a gas fluidized bed, Chem. Eng. Sci. 62 (2007) 356–370.
[20] D. Laskovski, P. Duncan, P. Stevenson, J. Zhou, K.P. Galvin, Segregation of hydraulically suspended particles in inclined channels, Chem. Eng. Sci. 61 (2006) 7269–7278.
[21] A.S. Lavine, Analysis of fully develop opposing mixed convection between inclined parallel plates, Wärme - und Stoffübertragung 23 (1988) 249–257.
[22] G. Okoth, S. Centikaya, J. Brueggemann, J. Thoeming, On hydrodynamic optimization of multi-channel counter-flow lamella settlers and separation efficiency of cohesive particles, Chem. Eng. Process. 47 (2008) 90–100.
[23] J.D. Kulick, J.R. Fessler, J.K. Eaton, Particle response and turbulence modification in fully developed channel flow, J. Fluid Mech. 202 (1994) 109–134.

List of symbols

p: static pressure
v: kinematic viscosity
u_i: instantaneous velocity
U_i: average mean flow velocity
u_i': turbulent velocity fluctuation
$\overline{u_i'u_j'}$: Reynolds-stress tensor
k: kinetic energy
ε: turbulence dissipation rate
G_k: generation of turbulence kinetic energy due to mean velocity gradients
G_b: generation of turbulence kinetic energy due to buoyancy
a_k: inverse effective Prandtl numbers for k
a_ε: inverse effective Prandtl numbers for ε
u_p: velocity of the particle
m_p: mass of the particle
g: gravity acceleration
r: radius of the particle
ρ_p: density of the dispersed phase
C_L: lift coefficient
V: magnitude of the relative velocity vector
$F_D(u - u_p)$: drag force per unit particle mass
d_p: particle diameter
μ: dynamic viscosity
C_D: drag coefficient
ρ: density of the fluid
Δt: time step
F_{other}: other interaction forces
F_x: additional acceleration (force/unit particle mass) term
Y_d: mass fraction of particles of diameter greater than d
n: size distribution parameter